Two-Way Procedure for Magnetostatic Finite Element Formulations via a Perturbation Method with Application to Thin Structures

Vuong Dang Quoc

Abstract— *In this paper, a perturbation finite element method with magnetostatic formulations is developed for treating errors occurring from thin structure models, that volume structures are considered as surfaces for 3-D model or surfaces are considered as lines for 2-D model. Nevertheless, these considerations generally ignore curvature effects next to corners and edges. The process of correction for thin shell assumption is performed with a two-way procedure that allows a full/complete problem to divide into several sub-domains including stranded inductors-thin magnetic structures and volume improvement. At the discrete level, each sub-domain is only solved on its own sub-mesh, generally distinct from the complete/full one. This allows reducing the degree of freedom in matrixes due to the reduced size of each sub-domain.*

Keywords— **Magnetostatics; magnetic scalar potential; magnetic field; thin structures; perturbation method.**

1. INTRODUCTION

In [1], a thin structure is considered a priori 1-D analytical distributions across the interface condition (IC). For that, the interior of volume thin regions is not meshed and is replaced by surfaces with impedance-type transmission conditions connected to the inner-analytical distributions. This neglects local distribution fields near edges and corners of shells, increasing with the thickness. To treat this disadvantage, the perturbation method for magneto-dynamic problems with the dual formulation has been recently proposed for one-way coupling [2]-[6].

In this researh, a novel scenario based on a perturbation method is proposed to accurately compute the magnetic scalar potential, magnetic flux density and magnetic field in volume correction starting from shell approximate solutions. The expanded method permits a full problem to split into sub-models with a two-way procedure (Fig. 1).

From this sub-model to another one is to be constrained via volume and surface sources expressed for material changes [2]-[6]. In each process, a sub-model is solved its own mesh and domain without depending on other sub-models, which permit to distinct from the complete one. The developments are developed for the ***h***-magnetostatic finite element formulations, paying special attention to the proper discretisation of the source constraints. The method is also validated on a practical problem to indicate the efficiency and differences.

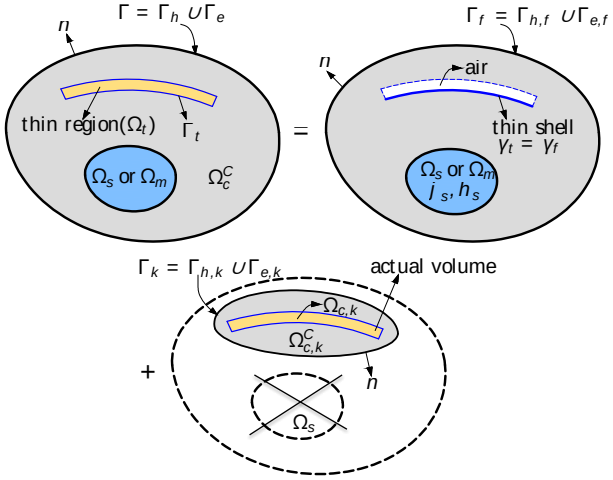

Fig. 1. Modeling of decompostion of a complete domain into several sub-models.

2. SERIES OF PERTUBATION METHOD

Canonical magnetostatic problem with surface and volume sources

A canonical magnetostatic problem n is defined is in a domain Ω_n, with boundary $\partial\Omega_n = \Gamma_n = \Gamma_{h,n} \cup \Gamma_{e,n}$, where subscripts n express as the associated sub-model n. The set of maxwell's equations, constitutive laws, boundary conditions (BCs), and ICs of the sub-model n expresses [6]-[8]

$$\text{curl}\, \boldsymbol{h}_n = \boldsymbol{j}_n, \text{div}\boldsymbol{b}_n = 0, \quad (1a\text{-}b)$$

$$\boldsymbol{b}_n = \mu_n \boldsymbol{h}_n + \boldsymbol{b}_{s,n} \quad (2)$$

$$\boldsymbol{n} \cdot \boldsymbol{b}_n|_{\Gamma_{e,n}} = 0, \ [\boldsymbol{n} \cdot \boldsymbol{b}_n]_{\gamma_n} = \boldsymbol{b}_{f,n} \quad (3a\text{-}b)$$

where $\boldsymbol{n}$ is the unit normal exterior to Ω_n.

The source field $\boldsymbol{b}_{s,n}$ in (2) is a volume source that accounts for fixing a remnant induction in magnetic materials or changes of permeability (μ_n) from the current problem to the next problem μ_m ($n \equiv m$), i.e.

Dang Quoc Vuong is with Training Center of Electrical Engineering, School of Electrical Engineering, Hanoi University of Science and Technology. Email: vuong.dangquoc@hust.edu.vn.

$$\boldsymbol{b}_{s,m} = (\mu_m - \mu_n)\boldsymbol{h}_n \quad (4)$$

The notation $[\cdot]_{\gamma_n} = |_{\gamma_n^+} - |_{\gamma_n^-}$. In (3 b) is the discontinuity of a quantity across the negative and positive sides (γ_n^+) and (γ_n^-). The field $\boldsymbol{b}_{f,n}$ is a surface source that accounts for special phenomena appearing in the idealized thin region between γ_n^+ and γ_n^- [2]-[5]. In addition, the magnetic field $\boldsymbol{h}_n$ in (1 a) is split in two parts $\boldsymbol{h}_{s,n}$ and $\boldsymbol{h}_{r,n}$, i.e.

$$\boldsymbol{h}_n = \boldsymbol{h}_{s,n} + \boldsymbol{h}_{r,n} \quad (5)$$

where $\boldsymbol{h}_{r,n}$ is the reaction field due to the magnetization of the magnetic materials and $\boldsymbol{h}_{s,n}$ is a source magnetic field generated by the imposed current density $\boldsymbol{j}_{s,q}$ such that

$$\text{curl}\, \boldsymbol{h}_{s,n} = \boldsymbol{j}_{s,n} \quad (6)$$

Procedure 1: Weak formuolation for inductor model and thin structure (SP n)

The magnetostatic weak formulation $(\boldsymbol{h}_n - \Phi)$ for procedure 1 (SP *n*) is obtained via the magnetic Gauss's law (1 b), i.e. [1]

$$-\int_{\Omega_n} \mu_n \boldsymbol{h}_{s,n} \cdot \text{grad}\Phi_n' d\Omega_n + \int_{\Omega_n} \mu_n \text{grad}\Phi_n \cdot \text{grad}\Phi_n' d\Omega_n + \int_{\Gamma_{e,n}} (\boldsymbol{n}\cdot\boldsymbol{b}_n)\cdot\Phi_n' d\Gamma_{e,n} - \gamma_n - \int_{\gamma_n} [\boldsymbol{n}\cdot\boldsymbol{b}_n]\cdot\Phi_n' d\gamma_n = 0, \forall \Phi_n' \in H_{h,n}^{10}(\Omega_n) \quad (7)$$

where $H_{h,n}^{10}(\Omega_n)$ is a function space presented in Ω_n including the basis functions for Φ_n as well as for the test function Φ_q'. The third surface integral in (7) is considered as a natural BC given in (3 a). The thin structure is defined via the last term in (7), i.e. [1]

$$-\int_{\gamma_n} [\boldsymbol{n}\cdot\boldsymbol{b}_n]\cdot\Phi_n' d\gamma_n = -\int_{\gamma_n} \mu_p d_p \boldsymbol{h}_{s,p} \cdot \text{grad}\Phi_n' d\gamma_n \quad (8)$$

By substituting (8) into (7), one has

$$-\int_{\Omega_n} \mu_n \boldsymbol{h}_{s,n} \cdot \text{grad}\Phi_n' d\Omega_n + \int_{\Omega_n} \mu_n \text{grad}\Phi_n \cdot \text{grad}\Phi_n' d\Omega_n - \int_{\gamma_n} \mu_p d_p \boldsymbol{h}_{s,p} \cdot \text{grad}\Phi_n' d\gamma_n = 0, \forall \Phi_n' \in H_{h,n}^{10}(\Omega_n) \quad (9)$$

Procedure 2: Weak formulation for volume corection (SP m)

The solution obtained from (9) is now corrected by a volume correction SP *m* via a volume source given by (2), i.e.

$$\boldsymbol{h}_m = \text{grad}\, \Phi_m,\ \boldsymbol{h}_n = \boldsymbol{h}_{s,n} - \text{grad}\Phi_n \quad (10a\text{-}b)$$

Hence, the weak form of SP *m* is:

$$\int_{\Omega_m} \mu_m \text{grad}\Phi_m \cdot \text{grad}\Phi_m' d\Omega_m - \int_{\Omega_m} (\mu_m - \mu_n)\text{grad}\Phi_n \cdot \text{grad}\Phi_m' d\Omega_m + \int_{\Omega_m} (\mu_m - \mu_n)((\boldsymbol{h}_{s,m} - \text{grad}\Phi_m') \cdot \text{grad}\Phi_m' d\Omega_m + \int_{\Gamma_{h,m}} (\boldsymbol{n}\cdot\boldsymbol{b}_m)\cdot\Phi_m' d\Gamma_{e,m} - \gamma_m - \int_{\gamma_m} [\boldsymbol{n}\cdot\boldsymbol{b}_m]\cdot\Phi_m' d\gamma_m = 0, \forall \Phi_m' \in H_{h,m}^{10}(\Omega_m) \quad (11)$$

At the discrete level, the source quantities Φ_n and $\boldsymbol{h}_{s,n}$ in (11) defined in SP *n* are also projected to the mesh of SP *m* via a projection method [9].

In addition, (11) needs to be remove representation of the shell discontinuity of SP *n* in SP *m* via the IC, i.e.

$$\int_{\gamma_m} [\boldsymbol{n}\cdot\boldsymbol{b}_m]\cdot\Phi_m' d\gamma_m = -\int_{\gamma_m} [\boldsymbol{n}\cdot\boldsymbol{b}_n]\cdot\Phi_m' d\gamma_m \quad (12)$$

Projection of solutions between two procedures

As presented above, the source fields Φ_n and $\boldsymbol{h}_n$ obtaining from the previous meshes of SP *n* are transferred to the mesh of SP *m*, i.e. [9]

$$(\boldsymbol{h}_{n,m-proj}, \boldsymbol{h}')_{\Omega_{s,m}} = (\boldsymbol{h}_n, \boldsymbol{h}')_{\Omega_{s,m}}, \forall \boldsymbol{h}' \in H_{h,m}^1(\Omega_{s,m}) \quad (13)$$

where $\forall \boldsymbol{h}' \in H_{h,m}^1(\Omega_{s,m})$ is curl-conform function space for the *m*-projected source $\boldsymbol{h}_{n,m-proj}$ (the projection of $\boldsymbol{h}_{m,m-proj}$ on mesh of SP *w*) and the test function $\boldsymbol{h}'$ defined on $\Omega_{s,m}$. For a magnetic scalar potential Φ_m, it can project the grad of Φ_n from the mesh of SP q, i.e. [9]

$$(\text{grad}\Phi_{n,m-proj}, \text{grad}\Phi')_{\Omega_{s,m}} = (\text{grad}\,\Phi_n, \text{grad}\Phi')_{\Omega_{s,m}} \quad \forall \Phi' \in H_{h,m}^{10}(\Omega_m) \quad (14)$$

where $\Phi' \in H_{h,m}^{10}(\Omega_m)$ is grad-conform function space for the *p*-projected source $\Phi_{n,m-proj}$ (the projection of Φ_n on mesh of SP *w*) and the test function Φ' defined on $\Omega_{s,m}$.

3. DISCRETIZATION OF FIELDS

For the magnetostatic case, the relation $\boldsymbol{h}_i = -\text{grad}\,\Phi_i\ (i = n\ or\ m)$ defines in the whole domain Ω_i. The scalar potential Φ_i is expressed as

$$\Phi_i|_{\Omega_i} = \Phi_{c,i}|_{\Omega_c^c} + \Phi_{d,i}|_{\Gamma_{cut,i}} + \Phi_{d,i}|_{\Gamma_{shell,i}} = \Phi_{c,i}|_{\Omega_c^c} + \sum_{i\in(\text{cut})} \Phi_{d,i}|_{\Gamma_{cut,i}} + \sum_{i\in(\text{shell})} \Phi_{d,i}|_{\Gamma_{shell,i}} \quad (15)$$

The discontinuous fields $\Phi_{d,i}|_{\Gamma_{cut,i}}$ and $\Phi_{d,i}|_{\Gamma_{shell,i}}$ are presented by restricting thier support to layers of elements to the positive side of the surface $\Gamma_{cut,i}$ and $\Gamma_{shell,i}$ [1], [7].

The field $\boldsymbol{h}_i$ can then be obtained from a scalar potential Φ_i everywhere in Ω_i. For that, the discretization of $\boldsymbol{h}_i - \Phi_i$ is now written as [1], [7].

$$\boldsymbol{h}_i = \boldsymbol{h}_{s,i} + \sum_{i \in N\left(\Omega_{c,i}^{C}\right)} \Phi_{c,n,i} v_{c,n,i} + \sum_{i \in shell} \left(\sum_{i \in N(\Gamma_{shell})} \Phi_{d,i} t_{d,n,i} \right) \quad (16)$$

where $v_{c,n,i}$ and $t_{d,n,i}$ are respectively expressed as

$$v_{c,n,i} = \sum_{\{p,q\} \in E\left(\Omega_{c,i}^{C}\right)} s_{e\{p,q\}} \quad (17)$$

$$t_{d,n,i} = \begin{cases} \sum_{\{p,q\} \in E\left(\Omega_{c,i}^{C}\right)} s_{e,\{p,q\}} \text{ in supp } (\Delta\Phi_{d,i}|_{\Gamma_{shell,i}}) \\ p \in N(\Gamma_{shell}), q \notin N(\Gamma_{shell}), q \in N_{shell,i}^{+} \\ 0 \text{ otherwise} \end{cases} \quad (18)$$

In (18), $q \in N_{shell,i}^{+}$ is the set of nodes of the transition layers supp $(\Delta\Phi_{d,i}|_{\Gamma_{shell,i}})$.

4. APPLICATION TEST

The practical application herein comprises a thin plate located on the right hand side of a stranded inductor. The magnetomotive force imposed in the stranded inductor is 1000 ampere-turns. The plate thickness is from 2 mm to 10 mm, for different relative permeabilities of $\mu_{r,plate}$ =300 and 500. The problem is tested in 2-D case.

As introduced in previous Sections, the test is implemented with a sequence including two procedures. A very fine mesh of the full/complte problem with more than 12 layers in the plate is shown in Figure 2. The colored map solutions on the magnetic scalar potential Φ of each sub-model are pointed out in Figure 3. A sub-model (SP *n*) attending with the stranded inductor and thin plate/shell without containing an actual volume is first solved in a coarch (Fig. 3,Φ_n, *top*). The volume correction that does not include the stranded inductor and thin plate anymore is given to improve the thin structure approximation (Fig. 3, Φ_m, *middle*) [1], [2]. Finally, the full/complete solution is a su sum of two previous solutions (SP *n* + SP *m*), for *d* = 10 mm and $\mu_{r,plate}$ = 500 (Fig. 3, $\Phi_{complte} = \Phi_n + \Phi_m$, *bottom*).

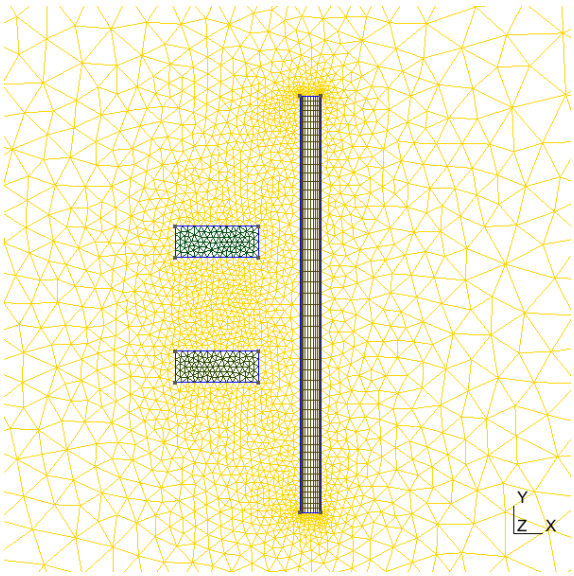

Fig. 2. Mesh of the complete problem.

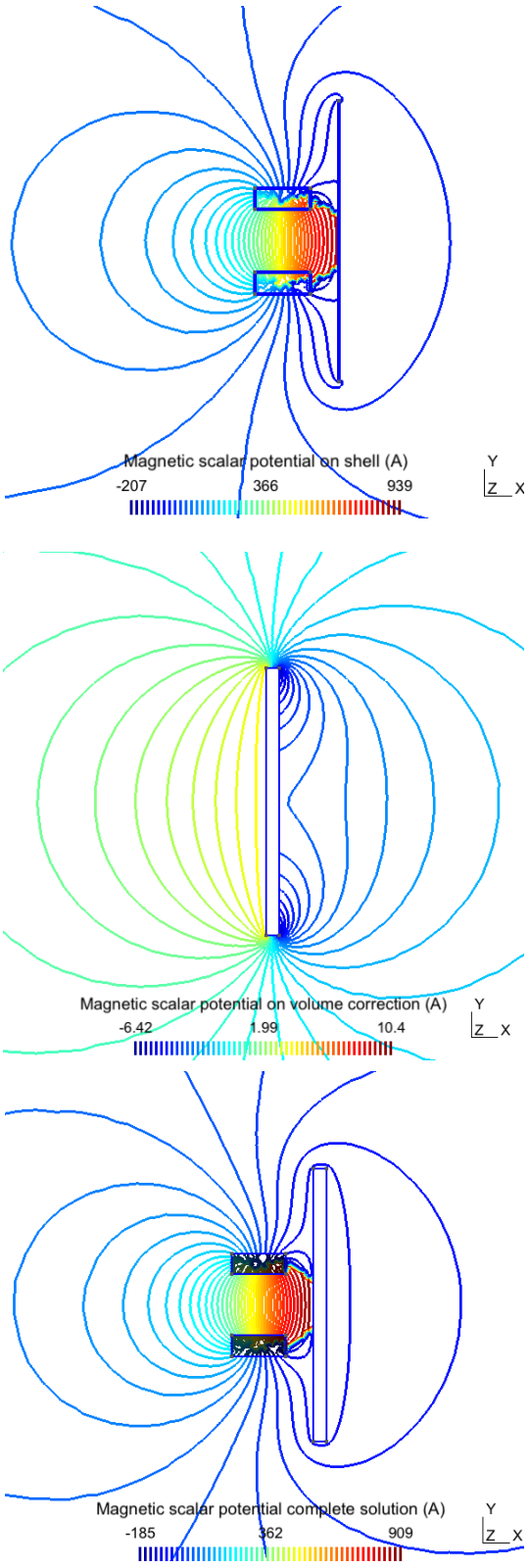

Fig. 3. Colored map of magnetic scalar potential distributions for the stranded inductors with the thin structure SP *n* (Φ_n, *top*), volume correction SP *m* (Φ_m, *middle)* and the full/complte solution ($\Phi_{complte} = \Phi_n + \Phi_m$, *bottom*), for a thickness *d* = 10 mm, $\mu_{r,plate}$ = 500).

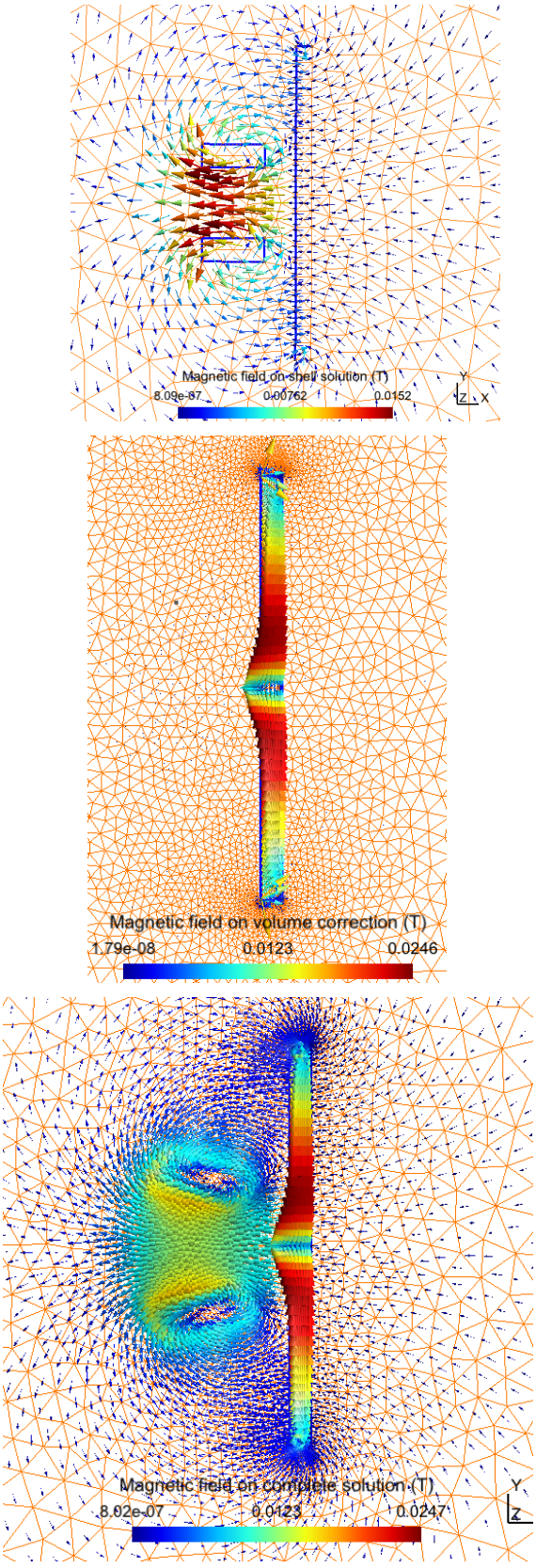

Fig 4. Magnetic flux density distributions $\boldsymbol{b} = \boldsymbol{\mu}(\boldsymbol{h}_s - \mathbf{grad}\,\boldsymbol{\Phi})$ for the stranded inductor and thin structure SP *n* (*top*), the volume improvement SP *m* (*middle*) and the full/complete solution (*bottom*) (*d* = 10 mm, $\mu_{r,plate}$ = 500).

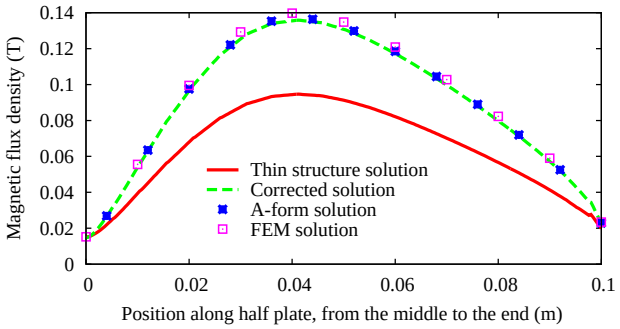

Fig 5. Magnetic flux density on TS solution and volume correction along the plate (*d* = 7.5mm).

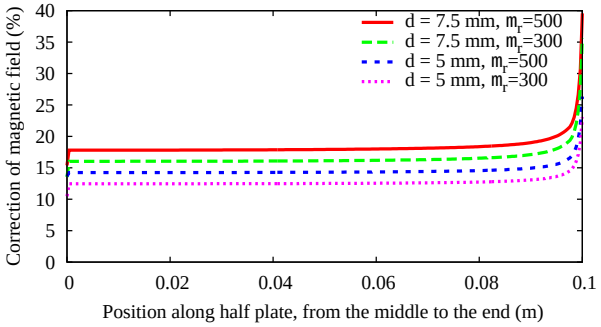

Fig 6. Correction of the magnetic field along the plate for different effects of *d* and μ_r.

In the similar way, the magnetic flux density distributions for each sub-model (sub-mesh) in computation from the different meshes is depicted in Figure 4, for d = 10 mm and $\mu_{r,plate}$ = 500. The shell solution $\boldsymbol{b}_n$ of SP *n* due to the source field $\boldsymbol{h}_{s,n}$ and grad Φ_n is presented with the coarse mesh (Fig. 4, *top*). The local mesh covering an actual volume and its vicinity is then shown (Fig. 4, *middle*) to correct errors of the shell solution $\boldsymbol{b}_n$. The complete solution in the full mesh solved by finite element method (FEM) [10] is next illustrated (Fig. 4, *bottom*).

Significant errors on the magnetic flux density between the thin shell solution (SP *n*) and local volume solution (SP *m*) along the plate are indicated in Figure 5, for *d* = 7.5 mm, $\mu_{r,plate}$ =500. The error reaches approximately 50% in vicinity of the plate end. The corrected solution is then compared with both the FEM solution and ***a***-form solution obtained from the computation in the FEM method [10] and the magnetic vector potential formulation [4], [5], [8]. The errors are less than 1 % for both cases.

The relative correction of the magnetic field along the plate is presented in Figure 6, for different thicknesses. It can reach several tens of percents in the surrounding plate, up to 47 % near edges and corners, for *d* = 7.5 mm, $\mu_{r,plate}$ =500. It reduces to be lower than 25 % for *d* = 5 mm and $\mu_{r,plate}$ =300.

5. CONCLUSION

In this contribution, a perturbation method for a two-procedure has been successfully presented with ***h***-conformal magnetostatic finite element formulations.

The local volumetric improvement (correction) has been fully proposed in the heart of the method to correct the inaccuracies of the magnetic scalar potential, magnetic flux density, and magnetic field near geometric discontinuities like edges and corners [1].

The obtained results of the developed method are validated to be quite similar to both the FEM solution and ***a***-form solution. This is also a very good demonstration between the studied technique and other methods [4], [5], [8]. [10]. In particular, this is also a good step to explode for a three-procedure in the next study.

All the procedures of the method have been successfully applied to the practical problem.

REFERENCES

[1] C. Geuzaine, P. Dular, W. Legros. 2000. Dual formulations for the modeling of thin electromagnetic shells using edge elements. *IEEE Trans. Magn*., vol. 36, no. 4, pp. 799–802.

[2] P. Dular, R. ; Sabariego. 2007. A perturbation method for computing field distortions due to conductive regions with *h*-conform magnetodynamic finite element formulations. *IEEE Trans. Magn.*, vol. 43, no. 4, pp. 1293-1296.

[3] Vuong.; Dang, P. Dular R.V. Sabariego, L. Krähenbühl, C. Geuzaine. 2013. Subproblem Approach for Modelding Multiply Connected Thin Regions with an h-Conformal Magnetodynamic Finite Element Formulation. *In EPJ AP.*, vol. 63, no.1.

[4] P. Dular, Vuong.; Dang, R.; Sabariego, L. Krahenbuhl and C. Geuzaine. 2011. Correction of Thin Shell Finite Element Magnetic Models via a Subproblem Method. *IEEE Trans. Magn.*, vol. 47, no. 5, pp. 1158–1161.

[5] Vuong.; Dang, P. Dular, R. V. Sabariego, L. Krahenbuhl, C. Geuzaine. 2012. Subproblem Approach for Thin Shell Dual Finite Element Formulations. *IEEE Trans. Magn*., vol. 48, no. 2, pp. 407–410.

[6] Vuong Dang Quoc, Chistophe Geuzaine. 2019. Using edge elements for mdoeling of 3-D Magnetodynamic Problem via a Subproblem Method. *Sci. Tech. Dev. J.* ; 23(1) :439-445.

[7] Dang Quoc Vuong, Nguyen Duc Quang. 2019. Coupling of Local and Global Quantities by A Subproblem Finite Element Method – Application to Thin Region Models. *Adv. Sci. Technol. Eng. Syst. J.* 4(2), 40-44.

[8] Vuong Dang Quoc and Christophe Geuzaine. 2020. Two-way coupling of thin shell finite element magnetic models via an iterative subproblem method. *COMPEL - The international journal for computation and mathematics in electrical and electronic engineering*. ahead-of-print. doi :10.1108/COMPEL-01-2020-0035.

[9] G. Parent, P. Dular, J.; Ducreux, F. Piriou. 2008. Using a galerkin projection method for coupled problems. Magnetics. *Trans. Magn.*, vol 44, no. 6, pp. 830–833.

[10] S. Koruglu, P. Sergeant, R.; Sabarieqo, Vuong.; Dang, M.; Wulf. 2011. Influence of contact resistance on shielding efficiency of shielding gutters for high-voltage cables. *IET Electric Power Applications*, vol.5, no.9, pp. 715-720.

NOMENCLATURE

The list of symbols used in this research is given below:

$\boldsymbol{h}_n$	Magnetic field (A/m)
$\boldsymbol{b}_n$	Magnetic flux density (T)
$\boldsymbol{j}_n$	Electric current density (A/m^2)
Φ	Magnetic scalar potential (A)
$\boldsymbol{b}_{s,n}$	Volume sources
$\boldsymbol{b}_{f,n}$	Surface source field
Ω_n	Bounded open set of E^3
Γ_n	Boundary of Ω_q ($\Gamma_q = \partial\Omega_q$)
μ	Magnetic permeability (H/m)
μ_r	Relative magnetic permeability